PROCEEDINGS OF SCIENCE

Lattice calculations at non-zero chemical potential: The QCD phase diagram

Owe Philipsen
Westfälische Wilhelms-Universität Münster
E-mail: ophil@uni-muenster.de

The so-called sign problem of lattice QCD prohibits Monte Carlo simulations at finite baryon density by means of importance sampling. Over the last few years, methods have been developed which are able to circumvent this problem as long as the quark chemical potential is $\mu/T \lesssim 1$. After a brief review of these methods, their application to a first principles determination of the QCD phase diagram for small baryon densities is summarised. The location and curvature of the pseudo-critical line of the quark hardon transition is under control and extrapolations to physical quark masses and the continuum are feasible in the near future. No definite conclusions can as yet be drawn regarding the existence of a critical end point, which turns out to be extremely quark mass and cut-off sensitive. Investigations with different methods on coarse lattices show the light-mass chiral phase transition to weaken when a chemical potential is switched on. If persisting on finer lattices, this would imply that there is no *chiral* critical point or phase transition for physical QCD. Any critical structure would then be related to physics other than chiral symmetry breaking.

8th Conference Quark Confinement and the Hadron Spectrum
September 1-6, 2008
Mainz. Germany

PoS(Confinement8)011

1. Introduction

The QCD phase diagram has been the subject of intense research over the last ten years. Once fully determined, it will locate the regions of different forms of nuclear matter in the parameter space spanned by temperature T and baryon chemical potential μ_B. Based on the fundamental property of asymptotic freedom, one expects at least three different regions: hadronic (low μ_B, T), quark gluon plasma (high T) and colour-superconducting (high μ_B, low T). For chemical potentials exceeding $\mu_B \gtrsim 1$ GeV, the situation may be more complicated with possible additional phases. [1]

Unfortunately, a quantitative calculation of the phase diagram from first principles is extraordinarily difficult. Since QCD is strongly coupled on scales $\lesssim 4$ GeV, lattice simulations are the only tool to eventually give reliable answers, provided that systematic errors are controlled. As we shall see, at present it is still a long way to achieve this goal. In fact, lattice investigations at finite density are hampered by the "sign problem", and only approximate methods are available that work at small quark densities, $\mu = \mu_B/3 \lesssim T$. [2, 3] This adds further systematic errors to those known from zero density thermodynamics, like finite volume and discretisation effects. Accordingly, in this contribution we shall only consider the quark hadron transition at small densities. The widely accepted expectation is for a finite density first order phase transition terminating in a critical endpoint, and an analytic crossover behaviour at $\mu = 0$ (cf. Fig. 2 (left)).

2. The sign problem and calculational methods for finite density

Quark fields enter the QCD partition function quadratically and can be integrated out to give

$$Z = \int DU \, [\det M(\mu)]^f \, \mathrm{e}^{-S_g[U]} \,. \tag{2.1}$$

However, straightforward Monte Carlo simulations at finite quark chemical potential are impossible. The Dirac operator obeys the hermiticity relation $\not{D}(\mu)^\dagger = \gamma_5 \not{D}(-\mu*)\gamma_5$, which means that for colour group SU(3) and real chemical potential, the fermion determinant is complex. This prohibits its use as a probability weight in Monte Carlo algorithms and is known as the "sign-problem". The same relation tells us that for imaginary chemical potentials, $\mu = i\mu_i$, or finite isospin chemical potential, $\mu_u = -\mu_d$, the fermion determinant is real positive and can be simulated just as for $\mu = 0$. There are a number of methods that circumvent the sign problem, rather than solving it. All of these introduce some degree of approximation. However, the systematic errors are rather different, thus allowing for powerful cross-checks. Reviews specialised on the technical aspects can be found in Refs. [2, 3].

2.1 Reweighting methods

An exact mathematical fix to the sampling problem is to rewrite the partition function as

$$Z = \int DU \, [\det M(0)]^f \left[\frac{\det M(\mu)}{\det M(0)}\right]^f \mathrm{e}^{-S_g[U]} = \left\langle \left[\frac{\det M(\mu)}{\det M(0)}\right]^f \right\rangle_{\mu=0} \sim \mathrm{e}^{-const.V} \,, \tag{2.2}$$

i.e. generate the ensemble with the real positive determinant at $\mu = 0$ and correct by multiplying everything with a reweighting factor. However, Monte Carlo simulations by importance sampling

only use a few configurations where the integrand is peaked to estimate the integral, and the sampling and target distributions will have their peaks at different positions in configuration space. This is not a problem as long as there is sufficient overlap between the distributions, but the overlap will get worse as μ/T gets larger. In order to increase the overlap when studying phase transitions, one may reweight in both temperature and chemical potential such as to stay on the critical line [4]. Another problem of reweighting methods is that because of the fluctuating sign in the reweighting factor, the signal is exponentially suppressed with volume, making finite size scaling analyses prohibitively expensive.

2.2 Taylor expansion in μ/T

An alternative way to gain insight into the region of small density is to Taylor-expand observables around zero density,

$$\langle O\rangle(\mu) = \langle O\rangle(0) + \sum_{k=1} o_k \left(\frac{\mu}{\pi T}\right)^{2k}. \tag{2.3}$$

The coefficients o_k are derivatives of the observable evaluated at zero density and can be calculated without sign problem. Note that only even powers of μ are appearing for observables without explicit μ-dependence, due to the CP symmetry of QCD. This method is conceptually and computationally safe. Its drawback is that one has to compute the coefficients one by one and does not have much control over the convergence until several coefficients are known. Moreover, the coefficients involve derivatives of the fermion determinant, which are increasingly complex expressions with delicate numerical cancellations in higher orders.

2.3 Imaginary chemical potential and analytic continuation

Here one employs the positivity of the determinant at imaginary $\mu = i\mu_i$ to simulate observables in a technically safe and straightforward way without further approximations. But in order to get back to real μ, one has to approximate the full observable by a fit to truncated Taylor series,

$$\langle O\rangle(\mu_i) = \sum_k o_k \left(\frac{\mu_i}{\pi T}\right)^{2k}. \tag{2.4}$$

This allows some control over the systematics, i.e. a check whether such a series converges or not. If a fit by a few terms is possible, analytic continuation is straightforward. The disadvantage of this method is that it is restricted to $|\mu_B| \lesssim 500$ MeV because of unphysical $Z(3)$-transitions in the imaginary direction. Also, convergence properties might be quite different in the real and imaginary directions for some observables.

2.4 The critical line $T_c(\mu)$

The first task when studying the QCD phase diagram is to identify the phase boundary, i.e. the critical coupling and thus $T_c(\mu)$. This has been done for a variety of flavours and quark masses using different methods. For a quantitative comparison one needs data at one fixed parameter set. Such a comparison is shown for the critical coupling in Fig. 1 (left), for $N_f = 4$ staggered quarks with the same action and quark mass $m/T = 0.2$ [5]. (For that quark mass the transition is first order along the entire curve). One observes quantitative agreement up to $\mu/T \approx 1.3$, after which the different results scatter. Thus, all methods appear to be reliable for $\mu/T \lesssim 1$, or $\mu_B \lesssim 500$ MeV.

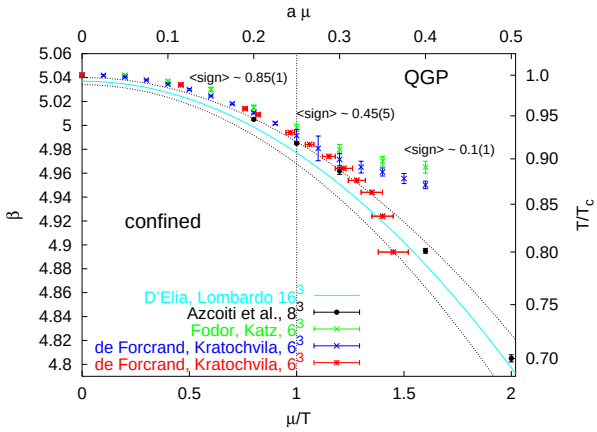

N_f	am	t_2	β-Function	Method	Ref.
2	0.1	0.69(35)	non-pert.	Taylor+Rew.	[6]
	0.032	0.500(54)	2-loop pert.	Imag.	[7]
3	0.1	0.247(59)	non-pert.	Taylor+Rew.	[6]
	0.026	0.667(6)	2-loop pert.	Imag.	[8]
	0.005	1.13(45)	non-pert.	Taylor+Rew.	[6]
4	0.05	1.86(2)	2-loop pert.	Imag.	[9]
2+1	0.0092,0.25	0.284(9)	non-pert.	Rew.	[10]

Figure 1: Left: Comparison of different methods to compute the critical couplings [5]. Right: Coefficient t_2 from the Taylor expansion of the transition line, Eq. (2.5), extracted on coarse lattices, $N_t = 4$.

The case of physical quark masses, after conversion to continuum units, is shown in Fig. 2 (left) [10]. One observes that T_c is decreasing only very slowly with μ. This is consistent with a description by a series in $(\mu/\pi T)^2$ with coefficients of order one,

$$\frac{T_c(\mu)}{T_c(0)} = 1 - t_2(N_f, m_f)\left(\frac{\mu}{\pi T}\right)^2 + \mathscr{O}\left(\left(\frac{\mu}{\pi T}\right)^4\right) \quad . \tag{2.5}$$

The leading coefficients for various cases have been collected from the literature [3] and are reproduced in Fig. 1. The curvature grows with N_f, which is consistent with $\sim N_f/N_c$ behaviour found in large N_c expansions [11]. Subleading coefficients are emerging at present but not statistically significant yet. Note that continuum conversions relying on the two-loop beta function are certainly not reliable for these coarse lattices, while fits to non-perturbative beta functions tend to increase the curvature, which otherwise falls significantly short of that of the experimentally observed freeze-out curve, $t_2 \approx 2.5$ [12].

3. Signals for a critical point

All calculational methods mentioned here also give signals for criticality. However, establishing those unambiguously is a much harder task and the comparison between the methods is difficult because different groups work with different actions and parameter sets. A simulation using reweighting methods was performed for quark masses tuned to give the ratios $m_\pi/m_\rho \approx 0.19, m_\pi/m_K \approx 0.27$, which are close to their physical values, on $N_t = 4$ lattices. The results put a critical point at $\mu_B^E \sim 360$ MeV [10], Fig. 2 (left), supporting the standard expected scenario for the QCD phase diagram. However, concerns have been raised about whether this critical point might be in the region where the reweighting method starts to be unreliable [13], hence a check of this result by other methods is desirable.

In principle the determination of a critical point is also possible via the Taylor expansion, where a true phase transition will be signalled by a finite radius of convergence for the pressure series about $\mu = 0$ as the volume is increased. The critical endpoint would thus signal the breakdown

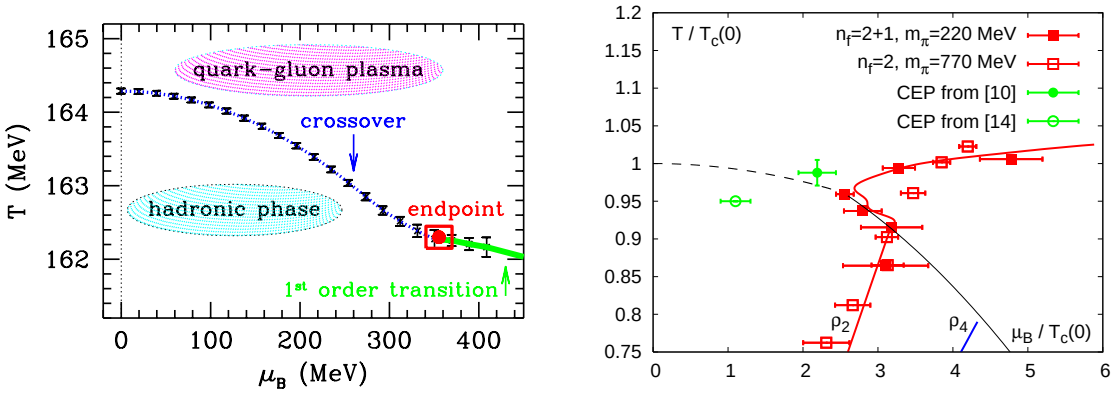

Figure 2: Left: Phase diagram from reweighting methods for physical quark masses on $N_t = 4$ [10]. Right: Estimated radius of convergence for the pressure on $N_t = 4$ [15].

of the Taylor series. One possible definition is

$$\frac{p}{T^4} = \sum_{k=1} c_k \left(\frac{\mu}{\pi T}\right)^{2k}, \quad \frac{\mu_E}{T_E} = \lim_{k\to\infty} \left(\left| \frac{c_k}{c_{k+1}} \right| \right)^{1/2}, \tag{3.1}$$

where the radius of convergence is given by the asymptotic ratio of Taylor coefficients. A critical endpoint for the $N_f = 2$ theory, based on this approach was reported in [32] for bare quark mass $m/T_c = 0.1$. Taking the measured first four coefficients for the asymptotic behaviour of the series, the estimate for the location of the critical point is $\mu_B^E/T_E = 1.1 \pm 0.2$ at $T_E/T_c(\mu = 0) = 0.95$. Similarly, Fig. 2 (right) shows estimates for the $N_f = 2+1$ theory with quark masses near physical, based on three consecutive coefficients [15]. While the calculations of Taylor coefficients at zero density are safe, the extraction of the critical signal might be problematic. There are other definitions for the radius of convergence, which all agree asymptotically but not when only a few coefficients are at hand. Also, it is known from the study of spin models that in some cases this method works remarkably well, but in others several ten coefficients are needed before asymptotic behaviour sets in [16].

4. The chiral critical line and surface

Rather than trying to tune the quark masses as close to their physical values as possible and switch on μ, a more general strategy is to explore the occurence and nature of phase transitions in the extended parameter space $\{m_{u,d}, m_s, \mu, T\}$. Understanding this will also shed light on the mechanisms and interplay of chiral symmetry breaking and confinement. The qualitative situation at zero density is shown in Fig. 3 (left). In the limits of zero and infinite quark masses (lower left and upper right corners), order parameters corresponding to the breaking of a global symmetry can be defined, and one numerically finds first order phase transitions at small and large quark masses at some finite temperatures $T_c(m)$. On the other hand, one observes an analytic crossover at intermediate quark masses, with second order boundary lines separating these regions. A convenient observable to study the order of a phase transition is the Binder cumulant $B_4(X) \equiv \langle (X - \langle X \rangle)^4 \rangle / \langle (X - \langle X \rangle)^2 \rangle^2$,

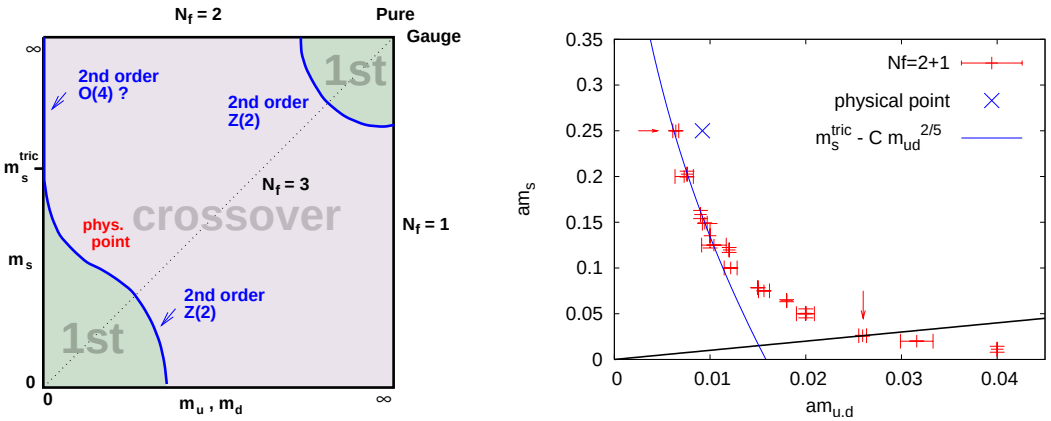

Figure 3: Left: Nature of the QCD phase transition as a function of quark masses, schematically. Right: The chiral critical line on an $N_t = 4$ lattice with staggered fermions [8].

with $X = \bar{\psi}\psi$. It is evaluated at the phase boundary, i.e. the temperature is tuned to its critical value for each quark mass combination. In the thermodynamic limit B_4 behaves as a step function, assuming the value 1 in a first order region and 3 in a crossover region, respectively. At a second order transition, B_4 assumes a critical value dictated by the universality class of the transition. On finite volumes the step function is smeared out to an analytic function whose approach to the thermodynamic limit has to be studied in a finite size scaling analysis. Both lines have been shown to belong to the $Z(2)$ universality class of the 3d Ising model [17, 18, 19], for which $B_4 = 1.604$.

4.1 The chiral critical line for $\mu = 0$

The boundary line for small quark masses is usually called the chiral critical line, as it bounds the quark mass region with a first order chiral phase transition. Starting from the case with three degenerate flavours, this line has been mapped out in [8], as shown in Fig. 3 (right). Indeed, the physical point is on the crossover side of the line, implying an analytic quark hadron transition for physical quark masses at zero density, as expected. The same conclusion is reached when analysing the nature of the transition at the physical point by finite size scaling and on a sequence of finer and finer lattices, such that a continuum extrapolation is feasible [20].

4.2 $N_f = 2$ at zero density

The situation is less clear for the chiral phase transition in the theory with two degenerate quarks in the upper left of Fig. 3 (left). The "derivations" of the generally expected QCD phase diagram [21] start with the assumption that the chiral transition for $N_f = 2$ is second order and thus in the $O(4)$ universality class, which implies the existence of a tricritical point at some strange quark mass m_s^{tric}. An extrapolation of the critical line in Fig. 3 (right) with the known tricritical (mean field) exponents would put it at $m_s^{tric} \sim 2.8T_c$. (This is on a coarse $N_t = 4$ lattice and quark masses receive large renormalisations on the way to the continuum.)

However, the nature of the $N_f = 2$ chiral transition is far from being settled. Wilson fermions appear to see O(4) scaling [22], while staggered actions are inconsistent with O(4) and O(2) (for the discretised theory) [23]. A recent finite size scaling analysis using staggered fermions with

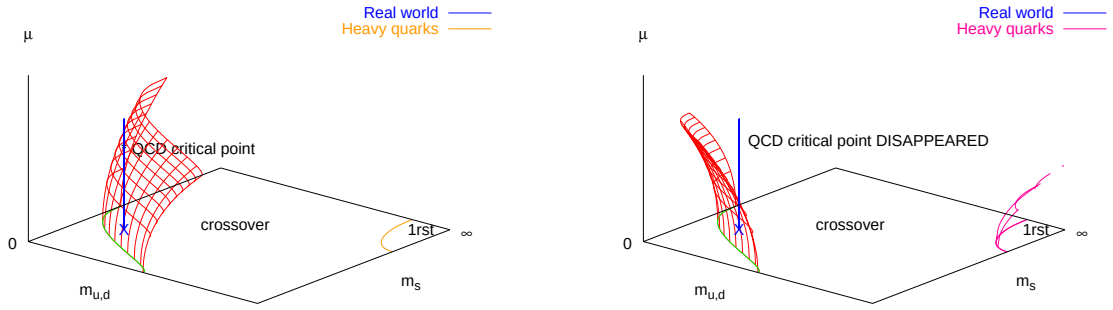

Figure 4: Extension of the chiral critical line to a critical surface for finite chemical potential. The expected QCD phase diagram is obtained for the case of positive curvature at zero density (left), while for negative curvature there is no chiral critical point (right).

unprecedented lattice sizes was performed in [24]. Again, these data appear inconsistent with O(4)/O(2), and the authors conclude a first order transition to be more likely. A different conclusion was reached in [25], in which χQCD was investigated numerically. This is a staggered action modified by an irrelevant term such as to allow simulations in the chiral limit. The authors find their data compatible with those of an $O(2)$ spin model on moderate to small volumes, which would indicate large finite volume effects in the other simulations. Finally, from universality of chiral models it is known that the order of the chiral transition is related to the strength of the $U_A(1)$ anomaly [26]. In a model constructed to have the right symmetry with a tunable anomaly strength, it has recently been demonstrated non-perturbatively that both scenarios are possible, with a strong anomaly required for the chiral phase transition to be second order [27]. Should the chiral transition turn out to be first order, the likely modification of Fig. 3 (left) would be the disappearance of the tricritical point, with the chiral critical line intersecting the $N_f = 2$ axis at some finite $m_{u,d}$ and being Z(2) all the way.

4.3 The chiral critical surface

When a chemical potential is switched on, the chiral critical line will sweep out a surface, as shown in Fig. 4. According to standard expectations [21], for small but non-zero $m_{u,d}$, the critical line should continuously shift with μ to larger quark masses until it passes through the physical point at μ_E, corresponding to the endpoint of the QCD phase diagram. This is depicted in Fig. 4 (left), where the critical point is part of the chiral critical surface. Note, however, that there is no a priori reason for this. In principle it is also possible for the chiral critical surface to bend towards smaller quark masses, cf. Fig. 4 (right), in which case there would be no chiral critical point or phase transition at moderate densities. For definiteness, let us specialise to the theory with three degenerate quarks, which lives on the diagonal in the quark mass plane. Similar to the critical temperature, the critical quark mass corresponding to the point on the chiral critical line can be expanded as as function of chemical potential,

$$\frac{m_c(\mu)}{m_c(0)} = 1 + \sum_{k=1} c_k \left(\frac{\mu}{\pi T}\right)^{2k} . \tag{4.1}$$

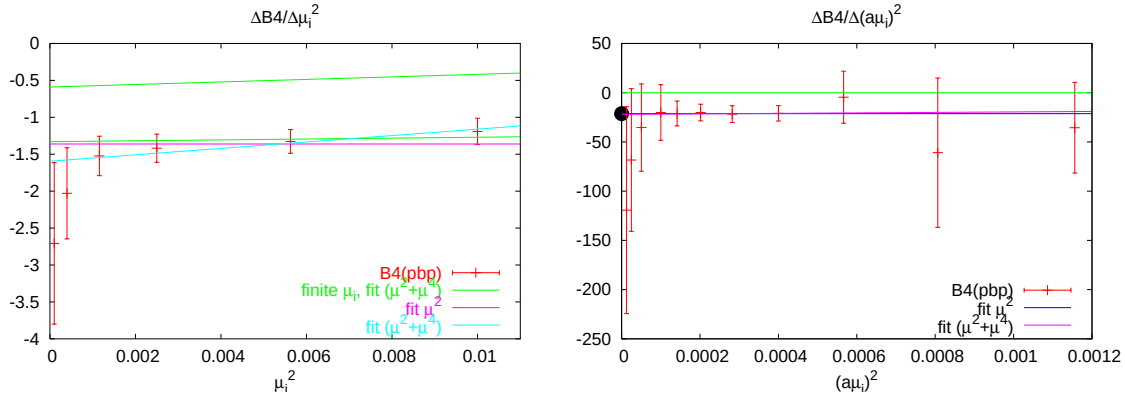

Figure 5: Curvature (in μ) of the Binder cumulant on the chiral critical line for $N_f = 3$ (left) [28] and $N_f = 2+1$ with physical strange quark mass (right).

A strategy to learn about the chiral critical surface is now to tune the quark mass to $m_c(0)$ and evaluate the leading coefficients of this expansion. In particular, the sign of c_1 will tell us which of the scenarios in Fig. 4 is realised.

The curvature of the critical surface in lattice units is directly related to the behaviour of the Binder cumulant via the chain rule,

$$\frac{dam_c}{d(a\mu)^2} = -\frac{\partial B_4}{\partial (a\mu)^2}\left(\frac{\partial B_4}{\partial am}\right)^{-1}. \tag{4.2}$$

While the second factor is sizeable and easy to evaluate in a simulation, the μ-dependence of the cumulant is excessively weak and requires enormous statistics to extract. In order to guard against systematic errors, this derivative has been evaluated in two independent ways. One is to fit the corresponding Taylor series of B_4 in powers of μ/T to data generated at imaginary chemical potential [8, 28], the other to compute the derivative directly and without fitting via the finite difference quotient [28]

$$\frac{\partial B_4}{\partial (a\mu)^2} = \lim_{(a\mu)^2 \to 0} \frac{B_4(a\mu) - B_4(0)}{(a\mu)^2}. \tag{4.3}$$

Because the required shift in the couplings is very small, it is adequate and safe to use the original Monte Carlo ensemble for $am_0^c, \mu = 0$ and reweight the results by the standard Ferrenberg-Swendsen method. Moreover, by reweighting to imaginary μ the reweighting factors remain real positive and close to 1. The results of these two procedures based on 20 and 5 million trajectories on $8^3 \times 4$, respectively, is shown in Fig. 5 (left). The error band represents the first coefficient from fits to imaginary μ data, while the data points represent the finite difference quotient extrapolated to zero. Both results are consistent, and the slope permits and extraction of the subleading μ^4 coefficient, while the combination of all data also constrains the sign of the μ^6 term. After continuum conversion the result for $N_f = 3$ is [28]

$$\frac{m_c(\mu)}{m_c(0)} = 1 - 3.3(3)\left(\frac{\mu}{\pi T}\right)^2 - 47(20)\left(\frac{\mu}{\pi T}\right)^4 - \dots. \tag{4.4}$$

The same behaviour is found for non-degenerate quark masses. Tuning to the physical strange quark mass on the critical line, i.e. to the point just left of the physical point in Fig. 3 (right), one

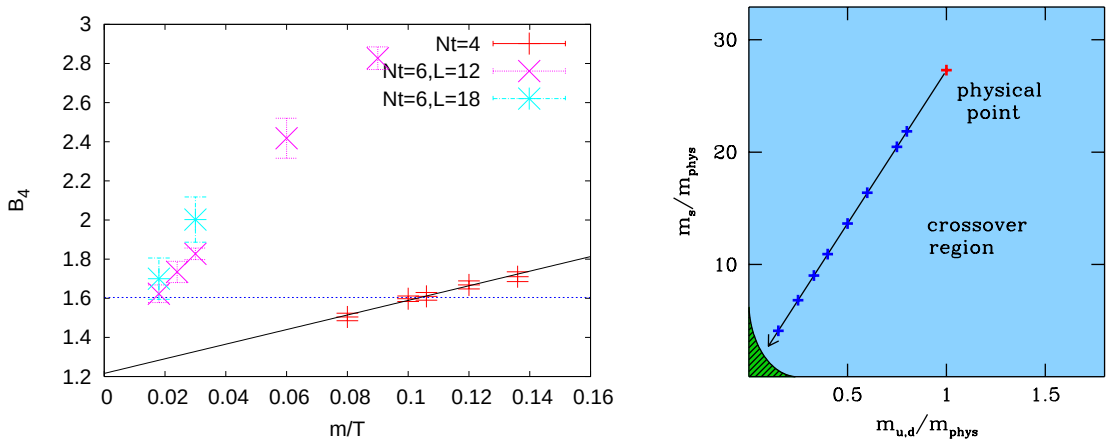

Figure 6: Left: Cut-off effects on the $N_f = 3$ critical mass $m^c(0)$ between $N_t = 4, 6$ [30]. Right: Shrinking of the first order transition region on finer lattices.

observes similar behaviour as shown in Fig. 5 (right), with a leading coefficient of about -24(11). Hence, on coarse $N_t = 4$ lattices, the region of chiral phase transitions shrinks as a real chemical potential is turned on, and there is no chiral critical point for $\mu_B \lesssim 600$ MeV.

4.4 Towards the continuum

The largest uncertainty in these calculations by far is due to the coarse lattice spacing $a \sim 0.3$ fm on $N_t = 4$ lattices. It is thus necessary to repeat all those studies on finer lattices. First steps in this direction are being taken with $N_t = 6, a \sim 0.2$ fm. Fig. 6 (left) shows a comparison of the critical quark mass for $\mu = 0$ in the $N_f = 3$ theory extracted for these cases. It is observed to dramatically shrink with decreasing lattice spacing [30]. The same observation is made for non-degenerate quark masses [31] and similarly for $N_f = 2$ [**?**]. Thus, in the continuum the gap between the physical point and the chiral critical line is much wider than on coarse lattices, as indicated in Fig. 6 (right). This demonstrates that on current lattices cut-off effects are much larger than finite density effects, and thus the results obtained so far should not yet be taken for continuum physics. Nevertheless, cut-off effects between $N_t = 4, 6$ appear to make a chiral critical point for moderate chemical potentials more unlikely, as it requires a very large positive curvature of the critical surface on the finer lattice.

5. Conclusions

The last few years have seen a lot of progress towards reliable lattice calculations for small quark chemical potentials $\mu/T \lesssim 1$. Finite density effects on the equation of state, screening masses and the critical temperature $T_c(\mu)$ are under control and continuum extrapolations for those quantities are feasible. A much more difficult task is the establishment of the order and nature of the quark hadron transition. On coarse lattices the chiral phase transition gets weakened with chemical potential, hence there is no chiral critical endpoint or phase transition for moderate densities $\mu_B \lesssim 600$ MeV. This does not exclude a critical point or phase transition that is not connected to chiral physics. Finer lattices are required to clarify these questions.

References

[1] K. Rajagopal and F. Wilczek, arXiv:hep-ph/0011333.

[2] O. Philipsen, PoS **LAT2005** (2006) 016 [PoS **JHW2005** (2006) 012] [arXiv:hep-lat/0510077].

[3] C. Schmidt, PoS **LAT2006** (2006) 021 [arXiv:hep-lat/0610116].

[4] Z. Fodor and S. D. Katz, JHEP **0203** (2002) 014 [arXiv:hep-lat/0106002].

[5] P. de Forcrand and S. Kratochvila, PoS **LAT2005** (2006) 167 [hep-lat/0509143].

[6] C. R. Allton *et al.*, Phys. Rev. D **66** (2002) 074507 [arXiv:hep-lat/0204010]. Nucl. Phys. Proc. Suppl. **129** (2004) 614 [hep-lat/0309116].

[7] P. de Forcrand and O. Philipsen, Nucl. Phys. B **642** (2002) 290 [arXiv:hep-lat/0205016].

[8] P. de Forcrand and O. Philipsen, JHEP **0701** (2007) 077 [hep-lat/0607017].

[9] M. D'Elia and M. P. Lombardo, Phys. Rev. D **67** (2003) 014505 [hep-lat/0209146].

[10] Z. Fodor and S. D. Katz, JHEP **0404** (2004) 050 [arXiv:hep-lat/0402006].

[11] D. Toublan, arXiv:hep-th/0510090.

[12] J. Cleymans *et al.*, Phys. Rev. C **73** (2006) 034905 [arXiv:hep-ph/0511094].

[13] K. Splittorff, arXiv:hep-lat/0505001; J. Han and M. A. Stephanov, arXiv:0805.1939 [hep-lat].

[14] R. V. Gavai and S. Gupta, Phys. Rev. D **71** (2005) 114014 [arXiv:hep-lat/0412035].

[15] C. Schmidt [for RBC-Bielefeld Collab.], J. Phys. G **35** (2008) 104093 [arXiv:0805.0236 [hep-lat]].

[16] J. M. Drouffe and J. B. Zuber, Phys. Rept. **102** (1983) 1.

[17] F. Karsch, E. Laermann and C. Schmidt, Phys. Lett. B **520** (2001) 41 [arXiv:hep-lat/0107020].

[18] P. de Forcrand and O. Philipsen, Nucl. Phys. B **673** (2003) 170 [arXiv:hep-lat/0307020].

[19] S. Kim *et al.*, PoS **LAT2005**, (2006) 166 [arXiv:hep-lat/0510069].

[20] Y. Aoki *et al.*, Nature **443** (2006) 675 [hep-lat/0611014].

[21] A. M. Halasz *et al.*, Phys. Rev. D **58** (1998) 096007 [arXiv:hep-ph/9804290]. M. A. Stephanov, K. Rajagopal and E. V. Shuryak, Phys. Rev. Lett. **81** (1998) 4816 [arXiv:hep-ph/9806219].

[22] A. Ali Khan *et al.* [CP-PACS Collaboration], Phys. Rev. D **63** (2001) 034502 [hep-lat/0008011]; Y. Iwasaki *et al.*, Phys. Rev. Lett. **78** (1997) 179 [hep-lat/9609022].

[23] C. W. Bernard *et al.* [MILC Collaboration], Phys. Rev. D **61** (2000) 111502 [hep-lat/9912018]; E. Laermann, Nucl. Phys. Proc. Suppl. **60A** (1998) 180.

[24] M. D'Elia, A. Di Giacomo and C. Pica, Phys. Rev. D **72** (2005) 114510 [hep-lat/0503030].

[25] J. B. Kogut and D. K. Sinclair, Phys. Rev. D **73** (2006) 074512 [hep-lat/0603021].

[26] R. D. Pisarski and F. Wilczek, Phys. Rev. D **29**, 338 (1984).

[27] S. Chandrasekharan and A. C. Mehta, [arXiv:0705.0617 [hep-lat]].

[28] P. de Forcrand and O. Philipsen, JHEP **0811** (2008) 012 [arXiv:0808.1096 [hep-lat]].

[29] M. Creutz, PoS **LATTICE2007** (2006) 007; A. S. Kronfeld, PoS **LATTICE2007** (2006) 016

[30] P. de Forcrand, S. Kim and O. Philipsen, PoS **LAT2007** (2007) 178 [arXiv:0711.0262 [hep-lat]].

[31] G. Endrodi *et al.*, PoS **LAT2007** (2007) 182 [arXiv:0710.0998 [hep-lat]].

[32] R. V. Gavai and S. Gupta, Phys. Rev. D **78** (2008) 114503 [arXiv:0806.2233 [hep-lat]].